Chinese Journal of Natural Medicines

Ustusolate E and 11 α –Hydroxy–Ustusolate E induce apoptosis in cancer cell lines by regulating the PI3K/AKT/mTOR and p–53 pathways

Mewlude Rehmutulla, Sitian Zhang, Jie Yin, Jianzheng Huang, Yang Xiao, Zhengxi Hu, Qingyi Tong, Yonghui Zhang

Citation: Mewlude Rehmutulla, Sitian Zhang, Jie Yin, Jianzheng Huang, Yang Xiao, Zhengxi Hu, Qingyi Tong, Yonghui Zhang, Ustusolate E and 11 α –Hydroxy–Ustusolate E induce apoptosis in cancer cell lines by regulating the PI3K/AKT/mTOR and p–53 pathways, Chinese Journal of Natural Medicines, 2025, 23(3), 346–353. doi: 10.1016/S1875–5364(25)60840–5.

View online: https://doi.org/10.1016/S1875–5364(25)60840–5

Chinese Journal of Natural Medicines 23 (2025) 346-353

Contents lists available at ScienceDirect

Chinese Journal of Natural Medicines

journal homepage: www.cjnmcpu.com/

Original article

Ustusolate E and 11α-Hydroxy-Ustusolate E induce apoptosis in cancer cell lines by regulating the PI3K/AKT/mTOR and p-53 pathways

Mewlude Rehmutulla[Δ], Sitian Zhang[Δ], Jie Yin, Jianzheng Huang, Yang Xiao, Zhengxi Hu[*], Qingyi Tong[*], Yonghui Zhang[*]

Hubei Key Laboratory of Natural Medicinal Chemistry and Resource Evaluation, School of Pharmacy, Tongji Medical College, Huazhong University of Science and Technology, Wuhan 430030, China

ARTICLE INFO

Article history:
Received 8 December 2023
Revised 23 April 2024
Accepted 6 May 2024
Available online 20 April 2025

Keywords:
Ustusolate E
11α-Hydroxy-ustusolate E
Cancer
PI3K/AKT/mTOR pathway
p-53 Pathway

ABSTRACT

Cancer represents a significant disease that profoundly impacts human health and longevity. Projections indicate a 47% increase in the global cancer burden by 2040 compared to 2020, accompanied by a further rise in the associated economic burden. Consequently, there is an urgent need to discover and develop new alternative drugs to mitigate the global impact of cancer. Natural products (NPs) play a crucial role in the identification and development of anticancer therapeutics. This study identified ustusolate E (UE) and its analog 11α-hydroxy-ustusolate E (HUE) from strain *Aspergillus calidoustus* TJ403-EL05, and examined their antitumor activities and mechanisms of action. The findings demonstrate that both compounds significantly inhibited the proliferation and colony formation of AGS (human gastric cancer cells) and 786-O (human renal clear cell carcinoma cells), induced irreversible DNA damage, blocked the cell cycle at the G_2/M phase, and further induced apoptosis in tumor cells. To the best of the authors' knowledge, this is the first report on the anticancer effects of UE and HUE and their underlying mechanisms. The present study suggests that HUE and UE could serve as lead compounds for the development of novel anticancer drugs.

1. Introduction

Cancer is a significant global public health challenge and one of the primary medical concerns to be addressed in the current century. According to the World Health Organization (WHO) estimates in 2019, cancer is the leading or second leading cause of death before the age of 70 in 112 countries [1]. The global cancer burden is projected to increase by 47% by 2040 compared to 2020 [1], further underscoring the escalating global burden of cancer. Gastric cancer (GC) is a common malignant tumor, reported to be the fifth most prevalent cancer and the fourth leading cause of cancer-related deaths globally [1, 2]. In contrast, kidney cancer (KC) exhibited an incidence of 431,288 new cases globally in 2020 [1]. Histologically, renal cell carcinoma (RCC) accounts for the vast majority (90%) of KC cases [3]. The incidence of KC exhibits gender dimorphism, with a higher prevalence in male populations. with KC being the 9th most common cancer among males and the 14th most common cancer among females [1]. Like most cancers, the development of GC and RC is multifactorial and long-lasting. Early-stage GC is underdiagnosed and more difficult to discover, which leads to the majority of patients being diagnosed only in the late stages of GC. This further contributes to the high mortality rate of GC. Conversely, more than 70% of RCC cases are incidentally diagnosed at the time of examination, with the remaining 30% presenting with advanced disease or metastases [4]. Cancer is a heterogeneous disease characterized by the dysregulation of multiple signaling pathways, leading to its complex molecular biology. This, in turn, affects cancer response to therapy and patient survival. While recognized and druggable targets exist, these targets are prone to mutation, and drug resistance is a common occurrence, rendering treatment efficacy unpredictable. Consequently, drugs with novel mechanisms of action are urgently needed as alternatives to mitigate the significant economic burden of cancer treatment globally.

The PI3K/AKT/mTOR signaling pathway regulates numerous cellular processes, including metabolism, motility, proliferation, growth, and survival. This pathway is among the most frequently dysregulated in human cancer [5]. Hyperactivation of the PI3K/AKT/mTOR pathway contributes to the expression of various hallmarks of cancer, such as evasion of apoptosis, induction of angiogenesis, tissue invasion and metastasis, and insensitivity to antigrowth signals [6, 7]. Therefore, this signaling cascade is considered a crucial target for the development of novel anti-cancer therapies.

The tumor suppressor protein p-53 is frequently absent or mutated in a significant proportion of cancers, estimated to be nearly half of all cases [8, 9]. When cells encounter stressors such as viral infection or DNA damage, p-53 becomes activated and binds to chromatin, initiating the transcription of downstream target genes to execute its tumor suppressive functions. These tumor-suppressive mechanisms are achieved through pathways such as cell cycle arrest and DNA repair [10]. Cell cycle checkpoints serve to monitor DNA replication during cell division. In the presence of irreparable DNA damage, these checkpoints can lead to cell cycle arrest and subsequent apoptosis [11]. Consequently, drugs targeting cell cycle-associated kinases or cell cycle checkpoints play a

* Corresponding author.
E-mail addresses: hzx616@126.com (Z. Hu); qytong@hust.edu.cn (Q. Tong); zhangyh@mails.tjmu.edu.cn (Y. Zhang)
Δ These authors contributed equally to this work.

https://doi.org/10.1016/S1875-5364(25)60840-5

crucial role in the treatment of various cancers and demonstrate promising prospects for further development.

Natural products (NPs) have played a highly significant role in the discovery and development of anticancer drugs [12-14]. Bicyclic sesquiterpenoids with a drimane skeleton represent a relatively minor group of NPs that are widely found in plants, geophytes, fungi, and some marine organisms, exhibiting diverse biological activities [15], such as relieving metabolic syndrome and demonstrating antitumor potential [16]. During a program aimed at discovering compounds with antitumor activity from an in-house NP library, two drimane sesquiterpenoids isolated from strain *A. calidoustus* TJ403-EL05 were identified as ustusolate E (UE) and 11α-hydroxy-ustusolate E (HUE), and were found to exhibit promising antitumor activity against AGS and 786-O cell lines [17]. Mechanistic research revealed that both compounds could significantly inhibit the proliferation and colony formation of AGS and 786-O cells, arrest the cell cycle at the G_2/M phase, and further induce apoptosis. These findings suggest that compounds HUE and UE could serve as lead compounds for the development of anti-GC therapeutics.

2. Materials and Methods

2.1. Fungal Material

Strain *A. calidoustus* TJ403-EL05 was isolated from wetland soil collected at East Lake, Wuhan City, Hubei Province, China, in July 2018 [18]. For identification purposes, the strain was cultured on potato dextrose agar (PDA) at 26 °C for seven days in an incubator. Afterward, the strain was identified based on morphological analysis and internal transcribed spacer (ITS) sequencing data of the rDNA. The ITS sequence data have been deposited in GenBank (accession number OM283555). The fungal sample was preserved at the culture collection center of Tongji Medical College, Huazhong University of Science and Technology.

2.2. Extraction and Isolation of UE and HUE

The fungal strain *A. calidoustus* TJ403-EL05 was cultured on PDA at 26 °C to prepare the seed cultures. Subsequently, the agar plugs were cut into smaller pieces and inoculated into 240 Erlenmeyer flasks (1 L), each containing 250 g of rice and 200 mL of distilled water, which were then sterilized by autoclaving. After incubation at 26 °C for 30 d, the fermented rice substrate was collected and extracted eight times with ethyl acetate at room temperature, yielding a crude extract (453 g). This extract was subjected to silica gel column chromatography, eluted with a gradient of petroleum ether and ethyl acetate (30∶1, 20∶1, 10∶1, 5∶1, 2∶1, 1∶1, and 0∶1, *V*/*V*), resulting in six major fractions (A–F). Fraction F (3.3 g) was further purified by reverse-phase liquid chromatography (RP-C_{18} CC) using a methanol-water gradient (20%–100%) to afford five main fractions (F1–F5). Fraction F4 (523.4 mg) was then purified by semi-preparative high-performance liquid chromatography (HPLC) using an acetonitrile-water mobile phase (60∶40, *V*/*V*; 2.0 mL·min^{-1}) to provide the compounds UE (8.4 mg, t_R = 35 min) and HUE (10.8 mg, t_R = 28 min). Compounds UE and HUE were stored at −20 °C and prepared from powder into a solution of the desired concentration before administration.

2.3. Cell Lines and Cell Culture

The AGS and 786-O cell lines were obtained from Procell (Wuhan, China). Both cell lines were maintained in DMEM/F12 medium supplemented with 10% fetal bovine serum (FBS) and incubated at 37 °C in a humidified environment with 5% CO_2.

2.4. Cell Viability Assay

Cell viability was assessed through the CCK-8 assay (TargetMol Chemicals, USA). Cells were seeded in 96-well plates at a density of 2000 cells per well. The following day, the cells underwent treatment with varying concentration gradients. After 48 h, 10 μL of CCK-8 reagent was added to each well, and the cells were co-cultured for an additional 2–3 h. Finally, the absorbance values at 450 nm were measured using a microplate reader [19].

2.5. Western Blotting (WB) Assay

Cell and tumor samples were collected and lysed in RIPA lysis buffer (Beyotime, Shanghai, China) supplemented with phenylmethylsulfonyl fluoride (PMSF, Beyotime, Shanghai, China) and phosphatase inhibitors (Vazyme, Nanjing, China). Protein concentrations were determined using a bicinchoninic acid (BCA) protein quantification kit (Beyotime, Shanghai, China). Equal amounts of protein from cell lysates were subjected to sodium dodecyl sulfate-polyacrylamide gel electrophoresis (SDS-PAGE) separation and transferred to nitrocellulose (NC) membranes. The membranes were blocked for 2 h at room temperature and incubated with primary antibodies overnight at 4°C. The primary antibodies used for immunoblotting are described in Table S1. Finally, the membranes were visualized using the Odyssey® CLx Imaging System (LI-COR) [20].

2.6. Apoptosis

Apoptosis was evaluated using the FITC Annexin V and PI Apoptosis Kit (ABP Biosciences, Wuhan, China), following the manufacturer's instructions. The proportion of FITC-positive cells was determined by flow cytometry (Becton Dickinson, CA, USA). Apoptosis analysis was conducted using FlowJo software version [21].

2.7. Cell Cycle Analysis

Cells were treated with vehicle control (DMSO, < 0.1%) or the compounds, then harvested and fixed in 70% ethanol for 12–14 h at 4 °C. After washing with cold PBS three times, the cells were resuspended in 200 μL of PI/Triton X-100 staining solution. Data were acquired using a flow cytometer (Becton Dickinson, CA, USA). The cell cycle distribution was determined using FlowJo software.

2.8. RNA Sequencing

Three biological replicates from the control (NC), HUE-treated (THUE), and UE-treated (TUE) groups were sequenced using the BGISEQ platform. Normalization and differential expression analysis were performed using the DESeq2 algorithm, with the following criteria applied: fold change greater than 1.5, *P*-value less than 0.05, and false discovery rate (FDR) less than 0.05. Detailed information on the differentially expressed genes (DEGs) identified by RNA-sequencing will be provided in the supplementary Tables S2 and S3. Visualization of the Kyoto Encyclopedia of Genes and Genomes (KEGG) pathway enrichment analyses and Gene Annotation and Enrichment Analysis (GAEA) was achieved using the BGI Dr. Tom platform (https://biosys.bgi.com/).

2.9. Reverse Transcription Quantitative Polymerase Chain Reaction (RT-qPCR)

Total cellular RNA was isolated using TRIzol™ Reagent (Thermo Fisher, USA, Cat: 15596026), and complementary DNA (cDNA) was synthesized using HiScript® II Q RT SuperMix for

qPCR (Vazyme, China, Cat: R223-01). SYBR Green qPCR Mix was purchased from Biosharp (Biosharp, China, Cat: BL698A). The primers employed are presented in Table S4.

2.10. Statistical Analysis

Data analysis was performed using GraphPad Prism 8 software. Statistical comparisons between the control and treatment groups were conducted. The results are expressed as mean ± standard deviation or standard error of the mean. One-way analysis of variance (ANOVA) was performed using GraphPad Prism 8.0, and differences were considered statistically significant at $^{*}P < 0.05$; $^{**}P < 0.01$; $^{***}P < 0.005$; $^{****}P < 0.001$.

Additional details regarding the materials and methods employed in this study are provided in the supplementary information.

3. Results

3.1. UE and HUE Inhibited the Proliferation of AGS GC and 786-O RCC Cell Lines

UE and its analog HUE are two drimane sesquiterpenoids (Fig. 1A). Previous studies have examined the antitumor activities of UE and HUE, on tumor cell lines such as AGS (gastric cancer), 786-O (renal cancer), SW480 (colorectal cancer), and HL-60 (leukemia). The results indicated that UE and HUE exhibited significant antitumor effects against the GC cell line AGS and the renal cancer cell line 786-O, with the anti-tumor impact on GC being particularly pronounced (Fig. 1B). The half-maximal inhibitory concentration (IC_{50}) values of UE for AGS and 786-O cells were 2.795 and 14.73 μmol·L^{-1}, respectively. The IC_{50} values of HUE in

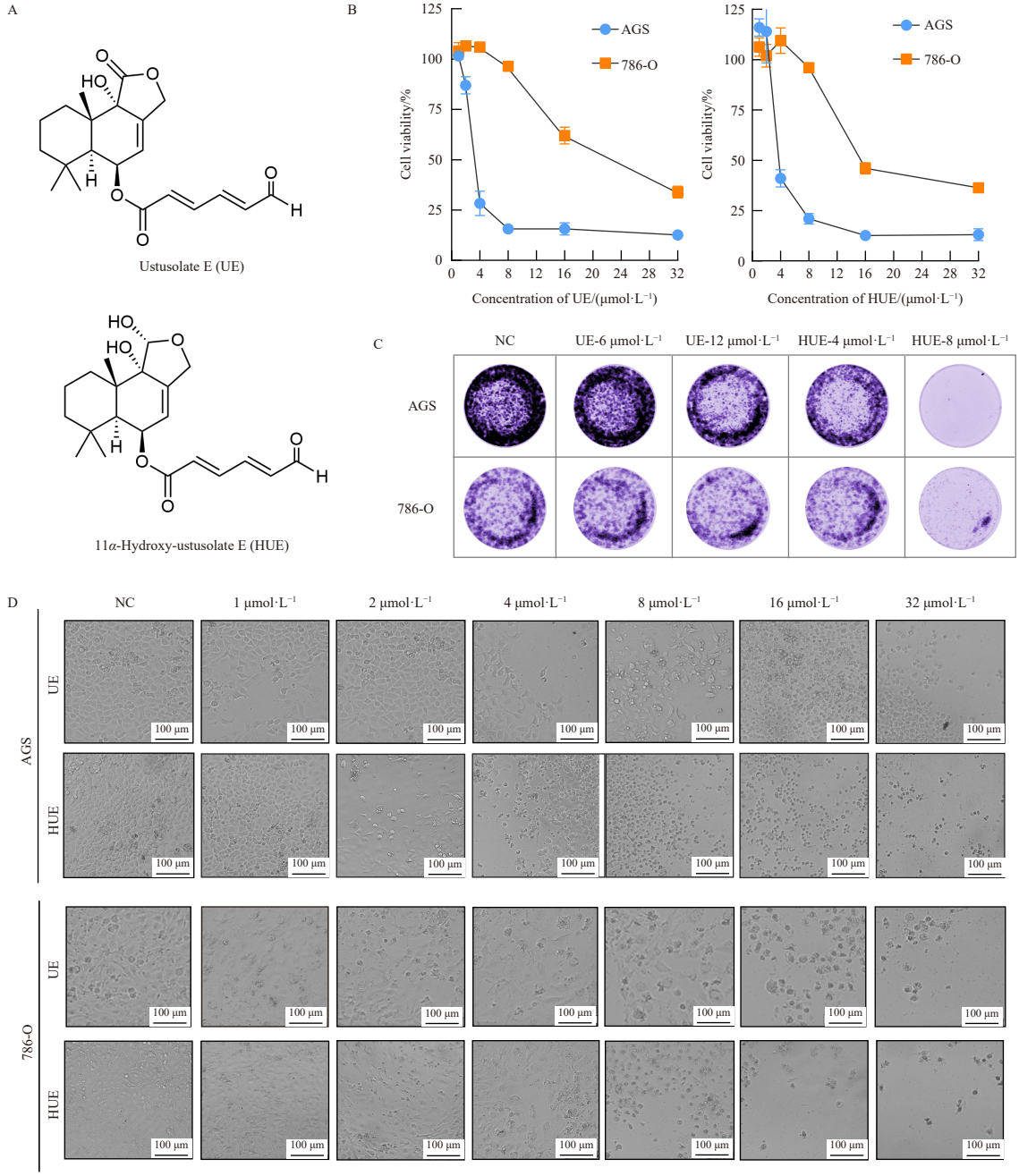

Fig. 1 UE and HUE inhibited the proliferation of AGS and 786-O. (A) Structures of UE and HUE. (B) Growth inhibition curves of UE and HUE on AGS and 786-O at 48 h. The data are presented as the mean ± SEM of three replicates. (C) AGS and 786-O were treated with UE (6, 12 μmol·L^{-1}) and HUE (4, 8 μmol·L^{-1}) and stained with crystal violet one week later. (D) Changes in cell morphology on AGS and 786-O with different concentrations of UE and HUE treatment, scale bar = 100 μm.

AGS and 786-O cells were 3.365 and 11.31 μmol·L^{-1}, respectively. The colony formation assay results demonstrated that both UE and HUE inhibited colony formation in a dose-dependent manner, with the analog HUE being more effective than UE in this regard (Fig. 1C). Microscopic observations further revealed that AGS cells treated with UE and HUE began to exhibit apoptosis at 2 μmol·L^{-1}, and nearly all cells were apoptotic at 16 μmol·L^{-1} (Fig. 1D). These findings suggest that UE and its analog HUE inhibited the proliferation of AGS and 786-O cells.

3.2. UE and HUE Inhibited the PI3K/AKT/mTOR Signaling Pathway

This study explored the effects of the compounds UE and its hydroxylated derivative (HUE) on the transcriptome of AGS cells. AGS cells were treated with UE (4 μmol·L^{-1}) and HUE (3 μmol·L^{-1}), and RNA was isolated after 24 h for RNA sequencing analysis. The results revealed that, when applying a fold change (FC) ≥ 1.5 and *Q*-value ≤ 0.05, the HUE-treated group (THUE) differed from the control group (NC) in the expression of 142 genes, with 96 upregulated and 46 downregulated (Fig. 2A). TUE differed from NC in the expression of 22 genes, with 16 upregulated and 6 downregulated (Fig. 2B). Mechanistic studies relied more on the THUE group because the two compounds had the same skeleton and THUE *vs* NC screened for more DEGs. Next, DEGs were subjected to functional enrichment analysis. KEGG pathway enrichment analysis showed that DEGs in the THUE group were significantly enriched in the focal adhesion, PI3K/AKT/mTOR signaling, and cell cycle pathways (Fig. 2C), while the DEGs in the TUE group were significantly enriched in cytokine-cytokine receptor interactions (Fig. 2D). Further investigation showed that HUE and UE did not affect focal adhesion, as indicated by the wound-healing assay results (Fig. S1). This finding suggests that HUE and UE do not affect focal adhesion. The PI3K/AKT/mTOR signaling pathway is a highly conserved major transduction network in all higher eukaryotic cells that promotes cell survival, growth and proliferation in response to external stimuli [22-24]. To confirm the effect of HUE and UE on the PI3K/AKT signaling pathway, AGS and 786-O cell lines were treated with HUE and UE, and the expression of p-PI3K, p-AKT, and p-mTOR was detected by Western blotting after 48 h. The results showed that p-PI3K, p-AKT, and p-mTOR appeared differentially downregulated after HUE and UE treatments compared to PI3K, AKT, and mTOR. This indicates that HUE and UE inhibited cancer cell proliferation by suppressing the PI3K/AKT/mTOR signaling

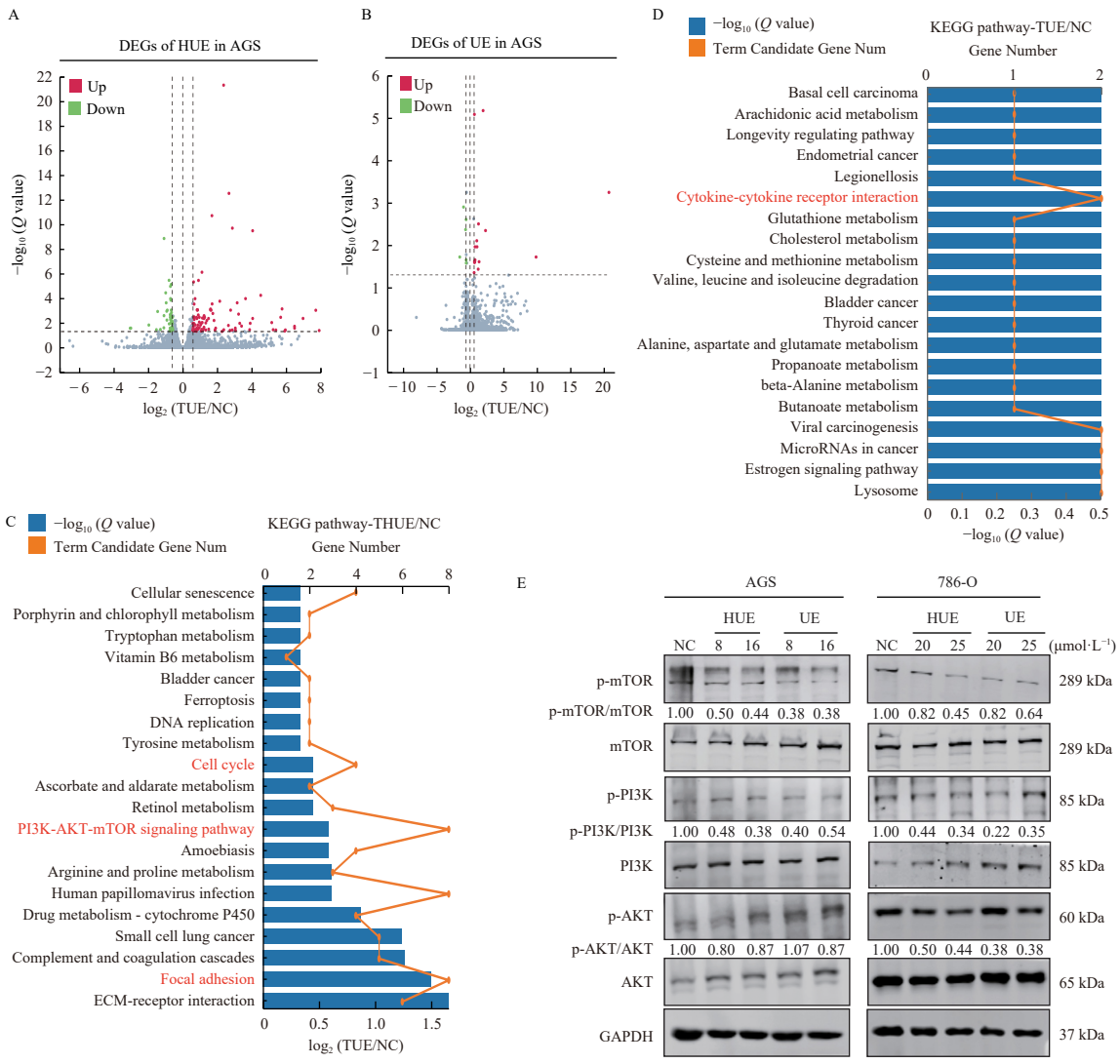

Fig. 2 UE and HUE inhibited the PI3K/AKT/mTOR signaling pathway. (A–B) Visualization of differential genes by volcano plot of AGS cells treated with HUE (3 μmol·L^{-1}, A) and UE (4 μmol·L^{-1}, B) for 24 h. Red points for up-regulated genes, green for down-regulated genes, and grey for unchanged genes (|log$_2$ FoldChange|> 1.5, P < 0.05). (C–D) Enrichment plots of DEGs on KEGG pathway in AGS cells treated with HUE (4 μmol·L^{-1}, C) and UE (8 μmol·L^{-1}, D) for 24 h. (E) Protein level of PI3K/AKT/mTOR pathway by Western blotting at 48 h.ing at 48 h.

pathway (Fig. 2E).

3.3. UE and HUE Led to DNA Damage and Activated the p-53 Signaling Pathway

To further investigate the effects of HUE and UE on downstream signaling pathways, a Gene Set Enrichment Analysis (GSEA) was performed. The results indicated that the p-53 pathway was activated following HUE and UE treatment (Figs. 3A–3B). To examine the changes in transcriptional levels of p-53 pathway-related genes, RT-qPCR was conducted. The analysis revealed upregulation of *14-3-3-σ*, *ATR*, *CHK1*, and *p21*, which are associated with the p-53 pathway (Figs. 3C–3D), suggesting the presence of DNA damage. To verify this, DNA damage-related proteins were detected using Western blotting. The results showed an increase in γ-H2AX protein expression after drug administration, indicating the occurrence of DNA damage. Further examination of DNA damage checkpoint-related proteins revealed upregulation of p-ATM, p-ATR, and p-CHK1, suggesting activation of DNA damage checkpoints. Concurrently, p-CDC2 protein expression was downregulated, implying a potential G_2/M cell cycle arrest (Fig. 3E).

3.4. UE and HUE Induce G_2/M Cell Cycle Arrest

The RNA-seq (Figs. 2C–2D) and Western blotting results (Fig. 3E) suggest that UE and its analog HUE may induce cell cycle arrest. To further investigate this, the cell cycle was examined by

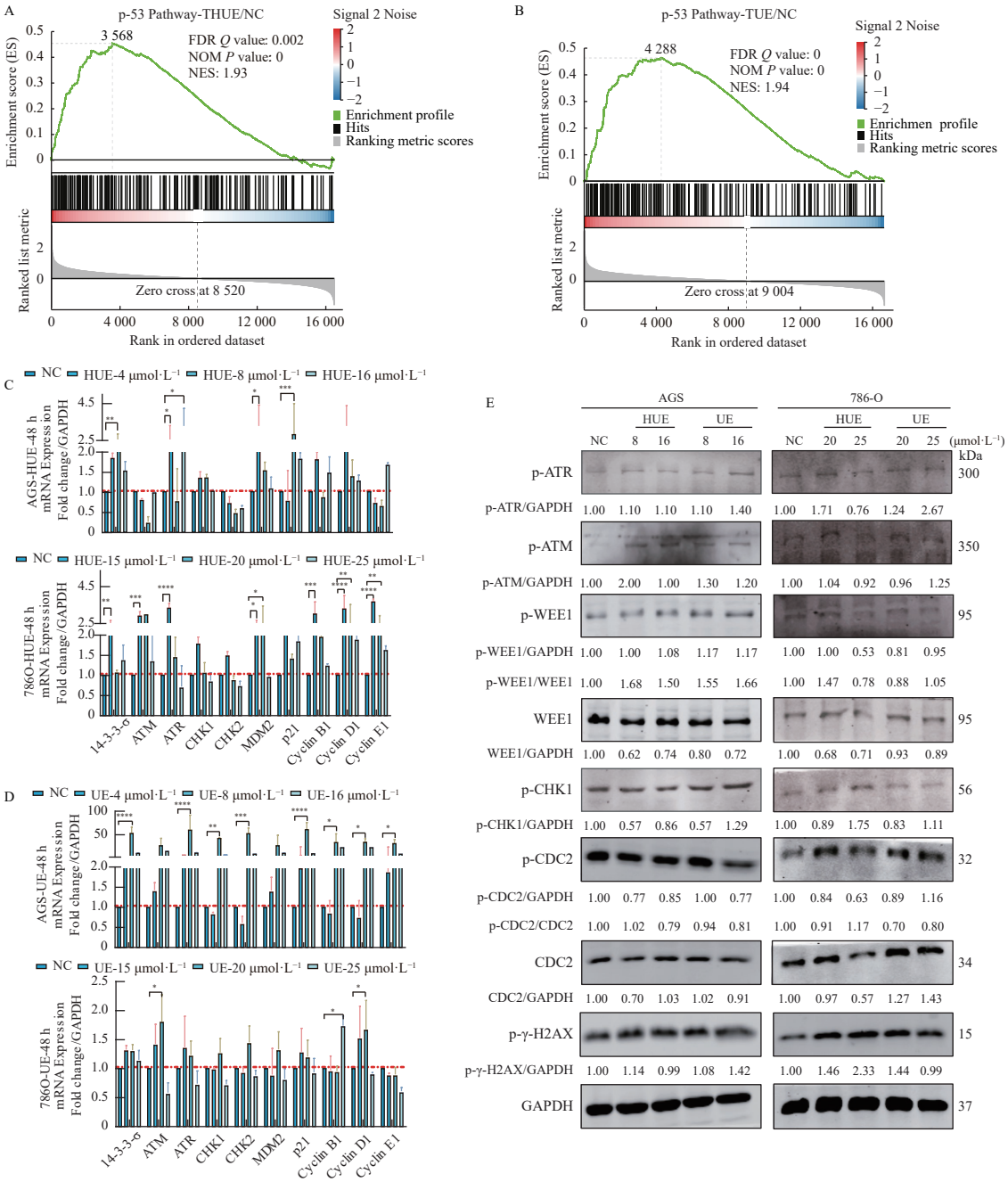

Fig. 3 UE and HUE led to DNA damage and activated the p-53 signaling pathway. (A–B) GSEA enrichment plots of DEGs on the p53 pathway in AGS cells treated with HUE (4 μmol·L^{-1}, A) and UE (8 μmol·L^{-1}, B) for 24 h. (C–D) AGS and 786-O were treated with HUE (C) and UE (D) for 48 h and then RT-qPCR was used to detect the level of p53 pathway-related genes. The data are presented as the mean ± SEM of three replicates. $^{*}P < 0.05$; $^{**}P < 0.01$; $^{***}P < 0.005$; $^{****}P < 0.001$. (E) Protein level of DNA damage checkpoint by Western blotting at 48 h.

flow cytometry (Figs 4A–4B). VP16 (5 μmol·L^{-1}) served as a positive control. The findings showed an increase in the G_2/M phase and a decrease in the S phase and G_0/G_1 phase, indicating G_2/M phase arrest after administration (Figs. 4C–4D). Western blotting analysis of cell cycle-related proteins revealed that CDK1 and Cyclin B1 were significantly downregulated, while CDK2, Cyclin A2, CDK4, and Cyclin D1 exhibited no significant changes (Fig. 4E). Since the CDK1 and Cyclin B1 complex promotes the transition from the premitotic phase to mitosis, the downregulation of these proteins suggests that the cells are unable to enter mitosis, resulting in cell cycle arrest.

3.5. UE and HUE-Induced Apoptosis

Previous research has established that apoptosis, or programmed cell death, is often induced subsequent to the onset of cell cycle arrest. Therefore, this study further examined the induction of apoptosis. The GSEA results indicated that genes associated with apoptotic processes appeared to be upregulated (Figs. 5A–5B). Flow cytometry analysis revealed that the compounds UE and its analog HUE induced significant apoptosis (Fig. 5C), with the effects comparable to the positive control drug doxorubicin (DOX) at a concentration of 1 μmol·L^{-1} (Figs. 5D–5E).

The findings indicated that, in addition to inducing cell cycle arrest, UE and its hydrogenated derivative (HUE) further promoted apoptosis and inhibited cancer cell proliferation (Fig. 5F). UE and HUE caused irreversible DNA damage in tumor cells, leading to the activation of the downstream DNA damage checkpoint ATM/ATR. The activated ATM/ATR then stimulated p53 and Chk1/Chk2, both of which inhibited CDC2 and Cyclin B, thereby blocking the tumor cells in the G_2/M phase. Concurrently, UE and HUE suppressed the PI3K/AKT/mTOR signaling pathway. Collectively, these mechanisms promoted apoptosis in the tumor cells.

4. Discussion

NPs and their analogs have demonstrated potent antitumor activity, making significant contributions to cancer therapeutics [25]. Compounds UE and HUE [26], derived from secondary metabolites of the wetland soil-derived fungus *A. calidoustus* TJ403-EL05, have been obtained . This suggests that HUE may also possess certain antitumor properties. Previous research has shown that HUE exhibited varying degrees of antitumor activity against a range of tumor cell lines, including AGS, 786-O, SW480, and HL-60 cells, with particularly notable effects on AGS and 786-O cells.

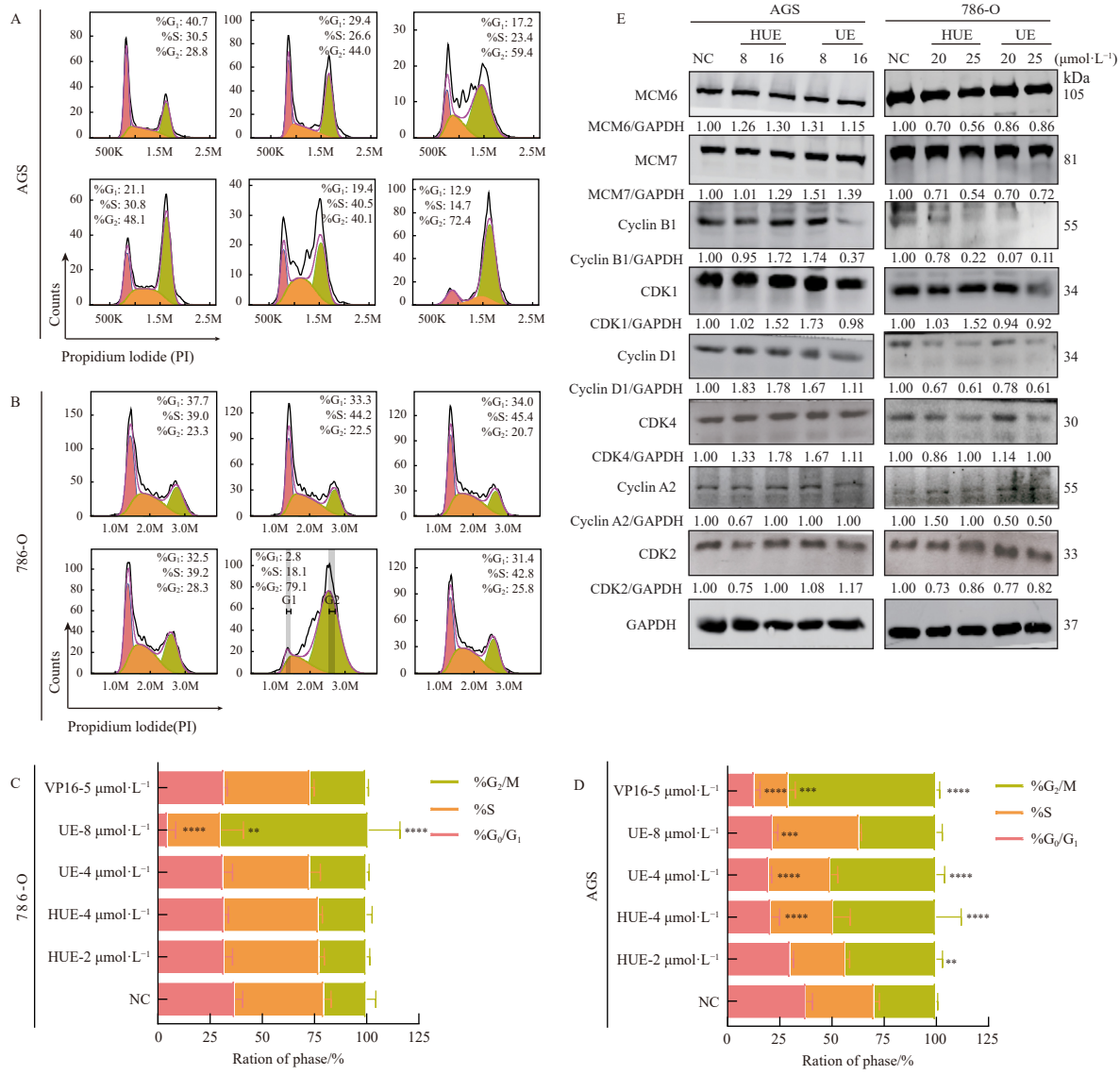

Fig. 4 UE and HUE caused G_2/M cell cycle arrest. (A–B) Flow cytometry was performed to detect UE- and HUE-induced cell cycle arrest in AGS cells (A) and 786-O cells (B) at 24 h. (C–D) Quantification of cell ratios at each phase of the cell cycle using GraphPad Prism 8 software. The data are presented as the mean ± SEM of three replicates. $^{**}P < 0.01$; $^{***}P < 0.005$; $^{****}P < 0.001$. (E) Protein level of cell cycle-related protein by Western blotting at 48 h.

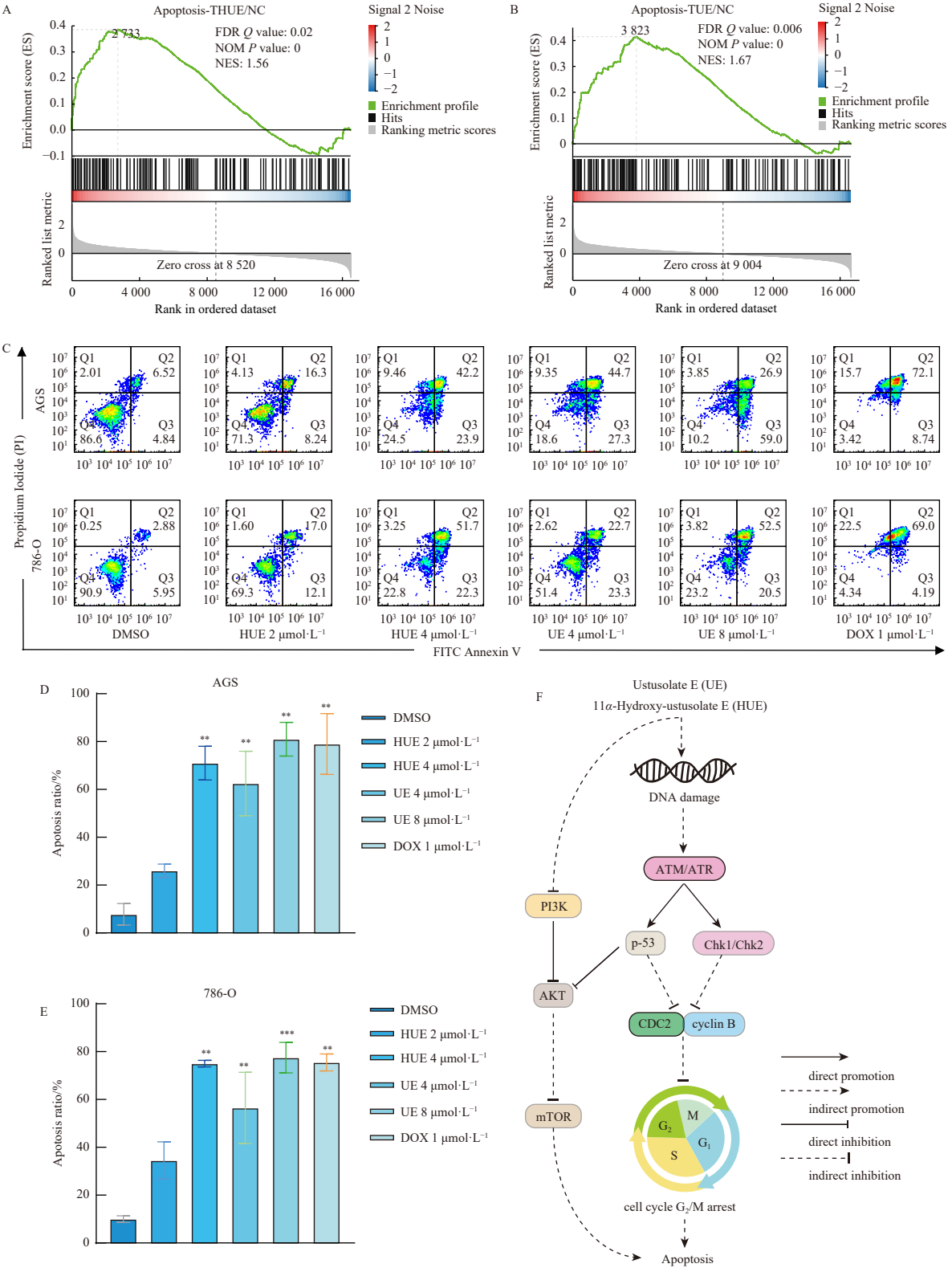

Fig. 5 UE and HUE-induced apoptosis. (A–B) GSEA enrichment plots of DEGs on apoptosis in AGS cells treated with HUE (4 μmol·L^{-1}, A) and UE (8 μmol·L^{-1}, B) for 24 h. (C) PI/Annexin V-FITC double-staining flow cytometry was performed to detect UE- and HUE-induced apoptosis in AGS and 786-O cells at 24 h. (D–E) Quantification of the positive cell ratio using GraphPad Prism 8 software. The data are presented as the mean ± SEM of three replicates. $^{**}P < 0.01$; $^{***}P < 0.005$. (F) Schematic model for the mechanism of UE and HUE.

Integrating the results from the cell proliferation inhibition assay and colony formation assay, it can be concluded that HUE presents superior antitumor activity.

The PI3K/AKT/mTOR signaling pathway is a highly conserved signal transduction network in eukaryotic cells that promotes cellular survival, growth, and proliferation [27]. As one of the most frequently activated pathways in cancer [28], the PI3K/AKT/mTOR cascade is a critical target for cancer therapeutics. This study's findings indicate that UE and its hydroxylated derivative (HUE) inhibit the PI3K/AKT pathway, leading to cellular apoptosis and the observed anticancer effects.

The p-53 gene regulates multiple components of the DNA

damage control response and promotes cellular senescence [29]. Exposures such as ultraviolet light, radiation, and certain medications can induce DNA damage. In response, cells possess DNA damage response (DDR) pathways and DNA repair proteins to address this damage [30]. Unrepaired DNA damage can promote cellular dysfunction [31]. Cell death pathways, such as apoptosis, play a central role in this process. The p-53 protein is a key factor in this mechanism, and high levels of DNA damage induce sustained p53 activation. The results of this study demonstrated that DNA damage checkpoint proteins, including ATM, ATR, and CHK1, were activated following UE and HUE treatments, leading to sustained p53 activation.

Mild DNA damage can be repaired with or without cell cycle arrest, while severe or irreparable damage leads to cell death [32]. Therefore, this study tested whether cell cycle arrest occurred after UE and HUE treatment, using VP16 as a positive control. VP16 is a semi-synthetic derivative of podophyllotoxin that inhibits DNA synthesis by inhibiting topoisomerase II activity, thereby enhancing double- and single-stranded cleavage of DNA and reversibly inhibiting topoisomerase II-bound repair [33]. The results indicate a significant increase in G_2/M phase cells after UE and HUE treatment, suggesting the occurrence of cell cycle arrest. Correspondingly, apoptosis was further detected, demonstrating that UE and HUE could cause significant apoptosis. Conversely, the positive control VP16 (5 μmol·L^{-1}) failed to produce significant cell cycle arrest in 786-O cells, which may be due to the cell line's relative insensitivity to VP16. The literature widely reports that VP16 has different IC_{50} values for different tumor cell lines [34], a phenomenon not discussed in depth here [34], and this phenomenon will not be discussed in depth here.

In summary, UE- and HUE-induced irreversible DNA damage arrested the cell cycle at the G_2/M phase by regulating the PI3K/AKT/mTOR and p-53 pathways, further inhibiting proliferation and inducing apoptosis in cancer cell lines. In conclusion, UE and HUE demonstrate the potential as lead compounds for the development of anticancer therapeutics.

Funding

This work was supported by the Program for Changjiang Scholars of the Ministry of Education of the People's Republic of China (No. T2016088), the National Natural Science Foundation for Distinguished Young Scholars (No. 81725021), the National Key R&D Program of China (No. 2021YFA0910500), the Science and Technology Major Project of Hubei Province (No. 2021ACA012), the Innovative Research Groups of the National Natural Science Foundation of China (No. 81721005), the Academic Frontier Youth Team of HUST (No. 2017QYTD19), and the Fundamental Research Funds for the Central Universities (No. 2172019kfyXJJS166).

Supporting Information

Supporting data can be requested by sending E-mail to the corresponding authors.

Declaration of competing interest

These authors have no conflict of interest to declare.

References

1 Sung H, Ferlay J, Siegel RL, et al. Global Cancer Statistics 2020: GLOBOCAN estimates of incidence and mortality worldwide for 36 cancers in 185 countries. *CA Cancer J Clin*. 2021;71(3):209-249. https://doi.org/10.3322/caac.21660.
2 Fattahi S, Amjadi-Moheb F, Tabaripour R, et al. PI3K/AKT/mTOR signaling in gastric cancer: epigenetics and beyond. *Life Sci*. 2020;262:118513. https://doi.org/10.1016/j.lfs.2020.118513.
3 Moch H, Cubilla AL, Humphrey PA, et al. The 2016 WHO classification of tumours of the urinary system and male genital organs-Part A: renal, penile, and testicular tumours. *Eur Urol*. 2016;70(1):93-105. https://doi.org/10.1016/j.eururo.2016.02.029.
4 Capitanio U, Montorsi F. Renal cancer. *Lancet*. 2016;387(10021):894-906. https://doi.org/10.1016/S0140-6736(15)00046-X.
5 Janku F, Yap TA, Meric-Bernstam F. Targeting the PI3K pathway in cancer: are we making headway? *Nat Rev Clin Oncol*. 2018;15(5):273-291. https://doi.org/10.1038/nrclinonc.2018.28.
6 Ul Islam B, Suhail M, Khan MS, et al. Flavonoids and PI3K/Akt/mTOR signaling cascade: a potential crosstalk in anticancer treatment. *Curr Med Chem*. 2021;28(39):8083-8097. https://doi.org/10.2174/0929867328666210804091548.
7 Tan AC. Targeting the PI3K/Akt/mTOR pathway in non-small cell lung cancer (NSCLC). *Thorac Cancer*. 2020;11(3):511-518. https://doi.org/10.1111/1759-7714.13328.
8 Finlay CA, Hinds PW, Tan TH, et al. Activating mutations for transformation by p53 produce a gene product that forms an hsc70-p53 complex with an altered half-life. *Mol Cell Biol*. 1988;8(2):531-539. https://doi.org/10.1128/mcb.8.2.531-539.1988.
9 Halevy O, Rodel J, Peled A, et al. Frequent p53 mutations in chemically induced murine fibrosarcoma. *Oncogene*. 1991;6(9):1593-1600.
10 Liu Y, Tavana O, Gu W. p53 Modifications: exquisite decorations of the powerful guardian. *J Mol Cell Biol*. 2019;11(7):564-577. https://doi.org/10.1093/jmcb/mjz060.
11 Matthews HK, Bertoli C, De Bruin RAM. Cell cycle control in cancer. *Nat Rev Mol Cell Biol*. 2022;23(1):74-88. https://doi.org/10.1038/s41580-021-00404-3.
12 Naeem A, Hu P, Yang M, et al. Natural products as anticancer agents: current status and future perspectives. *Molecules*. 2022;27(23):8367. https://doi.org/10.3390/molecules27238367.
13 Hu Q, Li Z, Li Y, et al. Natural products targeting signaling pathways associated with regulated cell death in gastric cancer: recent advances and perspectives. *Phytother Res*. 2023;37(6):2661-2692. https://doi.org/10.1002/ptr.7866.
14 Liu Y, Yang S, Wang K, et al. Cellular senescence and cancer: focusing on traditional Chinese medicine and natural products. *Cell Prolif*. 2020;53(10):e12894. https://doi.org/10.1111/cpr.12894.
15 Li F, Mo S, Yin J, et al. Structurally diverse metabolites from a soil-derived fungus *Aspergillus calidoustus*. *Bioorg Chem*. 2022;127:105988. https://doi.org/10.1016/j.bioorg.2022.105988.
16 Abu-Izneid T, Rauf A, Shariati MA, et al. Sesquiterpenes and their derivatives-natural anticancer compounds: an update. *Pharmacol Res*. 2020;161:105165. https://doi.org/10.1016/j.phrs.2020.105165.
17 Lu Z, Wang Y, Miao C, et al. Sesquiterpenoids and benzofuranoids from the marine-derived fungus *Aspergillus ustus* 094102. *J Nat Prod*. 2009;72(10):1761-1767. https://doi.org/10.1021/np900268z.
18 Zhang S, Mo S, Li F, et al. Drimane sesquiterpenoids from a wetland soil-derived fungus *Aspergillus calidoustus* TJ403-EL05. *Nat Prod Bioprospect*. 2022;12(1):27. https://doi.org/10.1007/s13659-022-00349-w.
19 Zhu H, Chen C, Tong Q, et al. Asperflavipine A: a cytochalasan heterotetramer uniquely defined by a highly complex tetradecacyclic ring system from *Aspergillus flavipes* QCS12. *Angew Chem Int Ed*. 2017;56(19):5242-5246. https://doi.org/10.1002/anie.201701125.
20 Yin J, Zhao Z, Huang J, et al. Single-cell transcriptomics reveals intestinal cell heterogeneity and identifies Ep300 as a potential therapeutic target in mice with acute liver failure. *Cell Discov*. 2023;9(1):77. https://doi.org/10.1038/s41421-023-00578-4.
21 Tong Q, You H, Chen X, et al. ZYH005, a novel DNA intercalator, overcomes all-trans retinoic acid resistance in acute promyelocytic leukemia. *Nucleic Acids Res*. 2018;46(7):3284-3297. https://doi.org/10.1093/nar/gky202.
22 Manning BD, Cantley LC. AKT/PKB signaling: navigating downstream. *Cell*. 2007;129(7):1261-1274. https://doi.org/10.1016/j.cell.2007.06.009.
23 Tian LY, Smit DJ, Jücker M. The role of PI3K/AKT/mTOR signaling in hepatocellular carcinoma metabolism. *Int J Mol Sci*. 2023;24(3):2652. https://doi.org/10.3390/ijms24032652.
24 Ahmad I, Hoque M, Alam SSM, et al. Curcumin and plumbagin synergistically target the PI3K/Akt/mTOR pathway: a prospective role in cancer treatment. *Int J Mol Sci*. 2023;24(7):6651. https://doi.org/10.3390/ijms24076651.
25 Atanasov AG, Waltenberger B, Pferschy-Wenzig EM, et al. Discovery and resupply of pharmacologically active plant-derived natural products: a review. *Biotechnol Adv*. 2015;33(8):1582-1614. https://doi.org/10.1016/j.biotechadv.2015.08.001.
26 Ogawa T, Uosaki Y, Tanaka T, et al. RES-1149-1 and -2, novel non-peptidic endothelin type B receptor antagonists produced by *Aspergillus* sp. III. Biochemical properties of RES-1149-1, -2 and structure-activity relationships. *J Antibiot (Tokyo)*. 1996;49(2):168-172. https://doi.org/10.7164/antibiotics.49.168.
27 Glaviano A, Foo ASC, Lam HY, et al. PI3K/AKT/mTOR signaling transduction pathway and targeted therapies in cancer. *Mol Cancer*. 2023;22(1):138. https://doi.org/10.1186/s12943-023-01827-6.
28 Yu L, Wei J, Liu P. Attacking the PI3K/Akt/mTOR signaling pathway for targeted therapeutic treatment in human cancer. *Semin Cancer Biol*. 2022;85:69-94. https://doi.org/10.1016/j.semcancer.2021.06.019.
29 Carson DA, Lois A. Cancer progression and p53. *Lancet*. 1995;346(8981):1009-1011. https://doi.org/10.1016/S0140-6736(95)91693-8.
30 Hoeijmakers JH. Genome maintenance mechanisms for preventing cancer. *Nature*. 2001;411(6835):366-374. https://doi.org/10.1038/35077232.
31 Roos WP, Kaina B. DNA damage-induced cell death by apoptosis. *Trends Mol Med*. 2006;12(9):440-450. https://doi.org/10.1016/j.molmed.2006.07.007.
32 Surova O, Zhivotovsky B. Various modes of cell death induced by DNA damage. *Oncogene*. 2013;32(33):3789-3797. https://doi.org/10.1038/onc.2012.556.
33 Van Maanen JM, Retèl J, De Vries J, et al. Mechanism of action of antitumor drug etoposide: a review. *J Natl Cancer Inst*. 1988;80(19):1526-1533. https://doi.org/10.1093/jnci/80.19.1526.
34 Zhao Y, Pu JX, Huang SX, et al. *ent*-Kaurane diterpenoids from *Isodon scoparius*. *J Nat Prod*. 2009;72(1):125-129. https://doi.org/10.1021/np800484j.